Toppling and height probabilities in sandpiles

Antal A. Járai Minwei Sun*

13th June 2019

Abstract

We study Abelian sandpiles numerically, using exact sampling. Our method uses a combination of Wilson's algorithm to generate uniformly distributed spanning trees, and Majumdar and Dhar's bijection with sandpiles. We study the probability of topplings of individual vertices in avalanches initiated at the centre of large cubic lattices in dimensions $d = 2, 3$ and 5. Based on these, we estimate the values of the toppling probability exponent in the infinite volume limit in dimensions $d = 2, 3$, and find good agreement with theoretical results on the mean-field value of the exponent in $d \geq 5$. We also study the distribution of the number of waves in 2D avalanches. Our simulation method, combined with a variance reduction idea, lends itself well to studying some problems even in very high dimensions. We illustrate this with an estimation of the single site height probability distribution in $d = 32$, and compare this to the asymptotic behaviour as $d \to \infty$.

JSTAT Keywords: Sandpile models, Avalanches, Critical exponents, Numerical simulations, Self-organized criticality
Additional Keywords: Wave, Uniform spanning tree, Wilson's algorithm, Exact sampling, Burning algorithm, Avalanche cluster size, Toppling probability

1 Introduction

1.1 Abelian sandpile model

We start with the definition of and some fundamental facts about the Abelian sandpile model on a finite graph G. Sandpiles are a lattice model of self-organized criticality, introduced by Bak, Tang and Wiesenfeld [1], and have been studied in both physics and mathematics. We refer to [2] for an overview. After discovering the Abelian group structure of addition operators in this model, Dhar [3] generalized it to arbitrary finite graphs and called it the Abelian sandpile model. He studied the self-organized critical nature of the stationary measure and gave an algorithmic characterization of recurrent configurations, the so-called "burning algorithm". This algorithm gives a one-to-one correspondence between the recurrent configurations of the Abelian sandpile models and rooted spanning trees [4]. This bijection is essential for our numerical simulations.

*Department of Mathematical Sciences, University of Bath, Claverton Down, Bath BA2 7AY, United Kingdom
Email: A.Jarai@bath.ac.uk, m.sun@bath.ac.uk

1.1.1 Basic properties

Let $G = (V \cup \{\rho\}, E)$ be a finite, connected graph, where we allow multiple edges between vertices. V is a finite set of vertices and the distinguished vertex ρ is called the *sink*. E is the set of edges and loop-edges are excluded for simplicity. Let $\deg_G(x)$ be the degree of the vertex x in the graph G and let $x \sim y$ denote that vertices x and y are connected by at least one edge.

Two examples we will be concerned with are as follows. Let $V \subset \mathbb{Z}^d$ be a finite d-dimensional box: $V = V_L = [-L, L]^d \cap \mathbb{Z}^d$. All vertices in $V^c = \mathbb{Z}^d \setminus V$ are identified to the sink, ρ. All loop-edges created at ρ are removed. This is called the *wired graph induced by* V. A second example is obtained, if we take $V = V_L \setminus \{s\}$, where $s = (L, \dots, L)$, with periodic boundary conditions. This is called the *torus graph*.

A *sandpile* is a collection of indistinguishable grains on the vertices in V. A sandpile is specified by a map $\eta : V \to \{0, 1, 2, \dots\}$. We say that η is stable at $x \in V$, if $\eta(x) < \deg_G(x)$ (the latter being $= 2d$ when $V \subset \mathbb{Z}^d$). We say that η is stable, if $\eta(x) < \deg_G(x)$, for all $x \in V$. Sometimes, especially in physics, a sandpile is specified by a map $\eta^* : V \to \{1, 2, \dots\}$. A stable sandpile is then defined as having one of the values $1, 2, \dots, \deg_G(x)$ at all x. This defines the same model after a trivial shift of coordinates.

If η is unstable (i.e. $\eta(x) \geq \deg_G(x)$ for some $x \in V$), x is allowed to topple which means that x passes one grain along each edge to its neighbours. When the vertex x topples, the grains are re-distributed as follows:

$$\begin{aligned} &\eta(x) \to \eta(x) - \deg_G(x); \\ &\eta(y) \to \eta(y) + n_{xy}, \quad y \in V, y \neq x. \end{aligned}$$

where n_{xy} is the number of edges between x and y. In the examples we are concerned with, we have $n_{xy} = 1$ for all $x, y \in V$. Grains arriving at ρ are lost, so we do not keep track of them. Toppling a vertex may generate further unstable vertices. Given a sandpile ξ on V, we define its stabilization

$$\xi^\circ \in \Omega_G := \{\textit{all stable sandpiles on V}\} = \prod_{x \in V} \{0, 1, ..., \deg_G(x) - 1\}$$

by carrying out all possible topplings, in any order, until a stable sandpile is reached. It was shown by Dhar [3] that the map $\xi \mapsto \xi^\circ$ is well-defined, that is, the order of topplings does not matter.

We now define the sandpile Markov chain with inital state η_0. The state space is the set of stable sandpiles, Ω_G. Fix a positive probability distribution p on V, i.e. $\sum_{x \in V} p(x) = 1$ and $p(x) > 0$ for all $x \in V$. Starting at $\eta \in \Omega_G$, choose a random vertex $X \in V$ according to p, add one grain at X and stabilize. The one step transition of the Markov chain moves from η to $(\eta + \mathbf{1}_\mathbf{X})^\circ$. Considering the sandpile Markov chain on a finite connect graph G, there is only one recurrent class [3]. We denote the set of recurrent sandpiles by $\mathcal{R}_G$.

1.2 Toppling probability exponent

Consider the stationary sandpile in the box $V_L = [-L, L]^d \cap \mathbb{Z}^d$ with Dirichlet boundary conditions. Let us add a grain at the origin o, and carry out the resulting avalanche. We are going to abbreviate the event 'when a grain is added at o, vertex x topples in the resulting

avalanche' to simply 'x topples'. Thus let $\mathbf{P}_L[x \text{ topples}]$ denote the probability that x topples in the avalanche initiated at o in volume V_L, and let $\mathbf{P}[x \text{ topples}] = \lim_{L\to\infty} \mathbf{P}_L[x \text{ topples}]$ be the infinite volume limit of this probability.

It was shown by Dhar [3], [2] that in the stationary sandpile in the box $V_L = [-L, L]^d \cap \mathbb{Z}^d$, the expected number of topplings at x, when a grain is added at o is given by the Green function $G_L(o, x)$ (the inverse of the graph Laplacian). In dimensions $d \geq 3$, this has infinite volume limit

$$\lim_{L\to\infty} G_L(o, x) = G(o, x) \sim c_d |x|^{2-d}, \quad \text{as } |x| \to \infty,$$

where we write $|x|$ for the Euclidean distance of x from o. Due to Markov's inequality, we have $\mathbf{P}[x \text{ topples}] \leq G(o, x)$. It was shown in [5] that in $d \geq 5$ it also holds that $\mathbf{P}[x \text{ topples}] \geq c\, G(o, x)$ with some constant $c = c(d) > 0$, and hence in these dimensions

$$\mathbf{P}[x \text{ topples}] \approx |x|^{2-d}. \tag{1.1}$$

In analogy with other statistical physics models at criticality (such as percolation at the critical threshold), the authors of [5] conjecture that in all dimensions $d \geq 2$ one has the behaviour

$$\mathbf{P}[x \text{ topples}] \approx |x|^{2-d-\eta} \tag{1.2}$$

with a critical exponent $\eta = \eta(d) \geq 0$. Then (1.1) shows that the mean-field value of η equals 0 ($d > 4$), and one expects that $\eta(d) > 0$ in dimensions $d = 2, 3$, and that $\eta(4) = 0$ with a logarithmic correction.

In this paper we carry out a numerical study of the conjecture (1.2) in dimensions $d = 2, 3$, and also study the behaviour of $\mathbf{P}_L[x \text{ topples}]|x|^{d-2}$ in $d = 5$. We also consider the scaling limit of the toppling probability $\mathbf{P}_L[x \text{ topples}]$ in finite volumes when $|x|/L$ is bounded away from 0.

1.3 Related work

To the best of our knowledge, individual toppling probabilities were not studied numerically previously in the literature. Manna [6] and Grassberger and Manna [7] studied average 'cluster sizes' related to our findings. In order to explain what these are, let

$$t_L(x; z) = \mathbf{P}_L[x \text{ topples if a grain is added at } z],$$

where $\mathbf{P}_L$ refers to probabilities in the stationary state in volume $[-L, L]^d$, with Dirichlet boundary conditions. Let us write $n(z, x)$ for the random variable that is the number of topplings at x, given a grain is added at z. The above papers considered the average number of topplings in an avalanche initiated at a randomly chosen site:

$$\langle s \rangle = \frac{1}{|V_L|} \sum_{z\in V_L} \mathbf{E}_L[\sum_{x\in V_L} n(z, x)] = \frac{1}{|V_L|} \sum_{z\in V_L} \sum_{x\in V_L} G_L(z, x) \sim c(d)L^2, \text{as } L \to \infty. \tag{1.3}$$

They also considered the average number of distinct sites toppled in such avalanches. This is given by an average over the vertex $z \in V_L$ where the avalanche is initiated of the expected number of $x \in V_L$ that topple at least once, that is, where $n(z, x) \geq 1$. Thus

$$\langle s_{\text{distinct}} \rangle = \frac{1}{|V_L|} \sum_{z\in V_L} \mathbf{E}_L[\sum_{x\in V_L} \mathbf{1}_{n(z,x)\geq 1}] = \frac{1}{|V_L|} \sum_{z\in V_L} \sum_{x\in V_L} t_L(x; z). \tag{1.4}$$

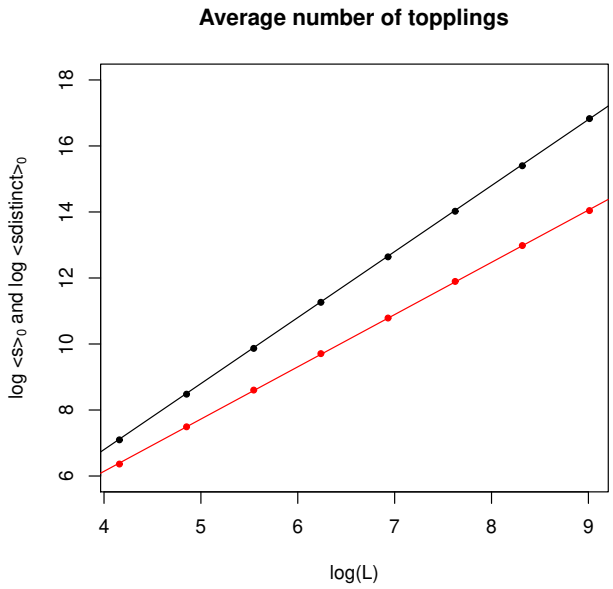

Figure 1: Log-log plot of average cluster size $\langle s \rangle_o$ (black) and average number of distinct sites toppled $\langle s_{\text{distinct}} \rangle_o$ (red) versus lattice size L with Dirichlet boundary conditions in $d = 2$, when considering $L = 2^n$ with $6 \leq n \leq 13$ with sample sizes 10^7, 10^7, 10^7, 10^7, 10^7, 2.5×10^6 and 6×10^5,6×10^5 respectively. The slope of the black line is 2, and the slope of the red line is 1.58.

In [7] it was found that this scales as $\approx L^{1.64}$ in $d = 2$. In order to confirm that our methods give results consistent with earlier work, we checked both of the exponents (1.3) and (1.4) with our simulation methods for lattice sizes comparable to those in [6] and [7] ($L = 64, 128, 256, 512$), and found very close agreement with the above exponents. Another test we performed was to check that our methods yield the exactly known height probabilities in 2D [8].

In the present paper we restrict to avalanches started at the origin o, which yield the somewhat modified average cluster sizes:

$$\langle s \rangle_o = \mathbf{E}_L[\sum_{x \in V_L} n(o,x)] = \sum_{x \in V_L} G_L(o,x) \sim c'(d) L^2, \text{as } L \to \infty. \tag{1.5}$$

and

$$\langle s_{\text{distinct}} \rangle_o = \mathbf{E}_L[\sum_{x \in V_L} \mathbf{1}_{n(o,x) \geq 1}] = \sum_{x \in V_L} t_L(x;o). \tag{1.6}$$

For the latter, we find an exponent somewhat different from that of (1.4), namely $\approx L^{1.58}$ in $d = 2$, when considering lattice sizes $L = 2^n$, $6 \leq n \leq 13$; see Figure 1.

The difference could be due to large avalanches started closer to the boundary having significantly smaller size than those started at the center of the box.

In 3D, Grassberger and Manna [7] found the behaviour of (1.4) to be very close to L^2, and suggest that the difference from (1.3) could be only a logarithmic correction. When we restricted to avalanches started at o, we found that (1.6) also differs very little from (1.5); see Figure 2. However, our analysis of individual toppling probabilities in 3D suggest that

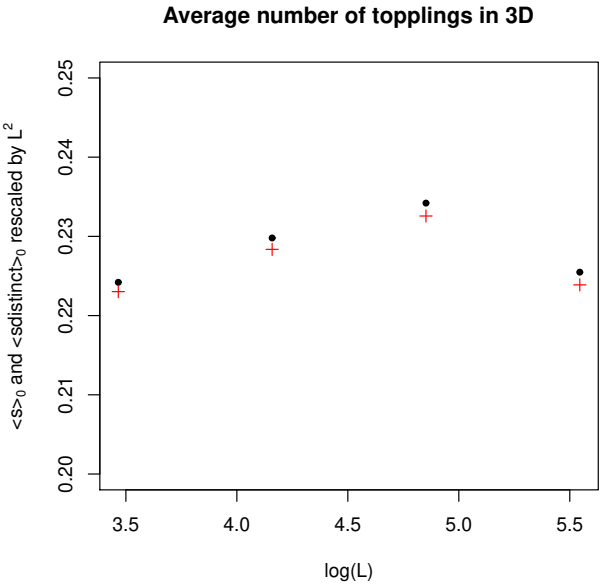

Figure 2: Average cluster size $\langle s \rangle_o$ and average number of distinct sites toppled $\langle s_{\text{distinct}} \rangle_o$ rescaled by L^2 versus $\log L$ with Dirichlet boundary conditions in $d = 3$. We considered the values $L = 32, 64, 128, 256$ (with sample sizes $10^7, 10^7, 4 \times 10^6$ and 4×10^5).

$\eta(3) > 0$ (≈ 0.09). The reason why this positive exponent does not affect the average number of topplings could be that the averages are dominated by very large avalanches.

We also collected data on the number of waves in 2D avalanches initiated at the origin. Let $w_L(n)$ be the probability of observing n waves in a box of radius L. It has been pointed out in [9] that although the expected scaling (in the limit $L \to \infty$) is $w(n) \sim n^{-2}$, the data is better fit with an exponent larger than 2 (about 2.1 in [9]). In Section 3.2, we present data restricting to avalanches initiated at the middle of the box, and see that there is better agreement with the theoretically predicted exponent 2 [4, Eqn. (5.11)].

Grassberger and Manna [7] observed that convergence to stationarity is faster, especially in high dimensions, starting from a uniformly random sandpile compared to an empty sandpile. As a partial explanation, in the present paper we state an asymptotic formula for the single site marginals in stationarity (and in the infinite volume limit) that approaches a uniform distribution as $d \to \infty$. We give the exact asymptotic formula for the probabilities of small heights given in terms of the Poisson distribution. Our asymptotic formula, whose proof will be published elsewhere, coincides with the asymptotics of the exact results of Dhar and Majumdar [10] on regular trees of high degree (see formula (8.2) in [10]).

2 Simulation methods

2.1 Overview

We use an exact sampling method. By this we mean that we use an algorithm that, given perfectly random numbers as input, will output a recurrent sandpile configuration that is *exactly* uniformly distributed (which is the steady-state of the model). First, we generate a

uniformly distributed spanning tree (or part thereof) on the underlying graph using Wilson's algorithm [11]. This is an efficient algorithm, and good estimates on its running time are available on cubic lattices. Note that since the number of spanning trees grows exponentially in the number of vertices, it is not a straightforward task to sample one uniformly at random. However, the algorithm in [11], described below, achieves this in polynomial time. Second, we convert the spanning tree into a sandpile configuration (or part thereof) based on a version of Majumdar and Dhar's burning bijection [4]. The sandpile configuration thus obtained is an unbiased sample from the stationary distribution of the model. This allows us to avoid any issues arising from having to estimate mixing properties of the underlying Markovian dynamics. A grain is added to the sampled configuration, and the resulting avalanche computed. The above is repeated a large number of times to obtain *independent* samples of avalanches in the steady-state. Independence allows us to estimate sampling errors accurately, and avoid issues arising from unknown effects due to correlated samples.

As random number generator, we used the 32 bit version of the Mersenne Twister [12], that is known to have a very large period ($> 2^{19,000}$). An additional advantage of this generator is that it allows one to 'jump ahead' by a given number of steps in the pseudo-random sequence [13], which allowed us to run computations in parallel with sequences that were guaranteed to be disjoint (we used jump-ahead with different multiples of 2^{100} steps on each node).

In 2D only about 44% of configurations yield an avalanche, and in high dimensions only about fraction $1/2d$. Therefore, in dimensions $d = 5$ and higher we used an importance sampling technique that allows us to sample only those configurations that yield an avalanche, and thereby increase the accuracy of our estimates compared to simple sampling. This is described in Section 2.3.

2.2 Wilson's algorithm

Let $G = (V \cup \{\rho\}, E)$ be a finite connected graph, where ρ plays the role of the sink for the sandpile. A loop-erased random walk (LERW) from vertex $x \in V$ with **target set** $F \ni \rho$ is defined as follows. Consider a simple random walk on G started from x and stopped at the first time it hits F. Then erase the loops in the path chronologically, as they are created, yielding a simple path between x and F. (When $x \in F$, we define this as the trivial path of zero steps.)

Wilson's algorithm generates a random spanning tree of G as follows. Enumerate the vertices in V as $V = \{x_1, \ldots, x_n\}$, and set $F_0 = \{\rho\}$. Run a LERW from x_1 with target set F_0, and let γ_1 be the path of the LERW. Set $F_1 = F_0 \cup \gamma_1$. Next, run a LERW from x_2 with target set F_1, and let γ_2 be the path of the LERW. Set $F_2 = F_1 \cup \gamma_2$, etc. The union of the loop-erased walks $\gamma_1, \ldots, \gamma_n$ form a random spanning tree of G. Wilson proved that the tree is uniformly distributed over all spanning trees of G [11], regardless of the chosen enumeration of V. Wilson also showed that the running time of the above algorithm is the mean commute time between ρ and a randomly chosen vertex that is distributed according to the stationary distribution of the simple random walk on G. Here the commute time between vertices x and y of G is defined to be $\mathbf{E}_x T_y + \mathbf{E}_y T_x$, where T_x is the first hitting time of x, and $\mathbf{E}_x$ is expectation over random walk started at x.

In our 2D simulations we used two different boundary conditions: (i) G is the $2L \times 2L$ torus with ρ equal one of the vertices (periodic boundary conditions); (ii) G is given by the box $V_L = [-L+1, L-1]^2$, with ρ equal to the entire boundary of this box (Dirichlet boundary

conditions). In case (i), the mean commute time between ρ and a random vertex of the torus is of order $L^2 \log L$; see [14, Proposition 10.13], and it is of the same order with the boundary condition (ii); see [14, Proposition 10.6]. Hence the entire spanning tree can be generated in time $O(L^2 \log L)$.

In 3D, we only used the Dirichlet boundary condition, and in this case the entire tree can be generated in time $O(L^3)$; see [14, Proposition 10.13].

In 5D and higher, avalanches typically take place on a small subset of the box. (The upper critical dimension for the model is $d_c = 4$; [15].) Hence on high-dimensional lattices we only generated those LERWs that were necessary to compute the avalanche; see Sections 2.3 and 2.4 below. The time required to compute a single LERW from the bulk of the lattice to the boundary is $O(L^2)$, as this is the number of random walk steps required. We used hashing [16, Sections 6.5,6.6] to store the generated random walk steps, and the resulting LERW, so the memory requirement for a single LERW is also $O(L^2)$. This method of simulation allowed us to investigate the height distribution at the origin in very high dimensions ($d = 32$), on lattices of radius up to $L = 128$, as this only requires running LERWs from the origin and its neighbours.

2.3 Bijection and importance sampling

We first recall Majumdar and Dhar's burning bijection [4]. Given a sandpile configuration η in volume V, first burn the sink vertex ρ. Then at each step $t \geq 1$, burn all vertices x such that

$$\eta(x) \geq \#\{\text{unburnt neighbours after step } t-1\}.$$

Let $B_t = \{x \in V : x \text{ burnt at step } t\}$. Connect a vertex in B_t to a neighbour in B_{t-1} by an edge. If there are more than one such neighbours, the choice can be made depending on the value of $\eta(x)$, in a bijective fashion. This maps the sandpile η to a spanning tree. In order to invert the map at a vertex x, it is sufficient to know the length of the paths in the spanning tree from x and its neighbours to ρ. For this purpose, when we generate our LERWs, we also record their lengths. Then the tree-distance $\mathrm{dist}(x, \rho)$ from any vertex x to ρ is given by the sum of the length of the LERW γ_x from x to its endpoint y in its target set and the tree-distance $\mathrm{dist}(y, \rho)$ from y to ρ. (This is already available when γ_x is generated, if we record the tree-distance along each LERW after they were generated.) We checked the one-site marginals obtained with the above method in 2D against the exactly known values [8], [17], [18], [19] and there was very close agreement.

We will need the following modification of the above burning rule [8]. Let us burn vertices as above, with the exception that the origin o is not allowed to burn. This way there will be a set $W \subset V$, such that $o \in W$, and W did not burn yet. Once only W is left unburnt, we burn o and complete the process by burning W. The following fact will be important. Let

$$q_d(i) = \mathbf{P}[\deg_W(o) = i], \quad i = 0, \ldots, 2d-1,$$

where $\deg_W(o)$ denotes the degree of vertex o in the subgraph of V induced by W, in other words, $\deg_W(o) = \#\{y \in W : y \sim o\}$. Then conditioned on the random variable $\deg_W(o)$, we have that the random variable $\eta(o)$ is uniformly distributed over the set $\{\deg_W(o), \ldots, 2d-1\}$ [8]. Then we have

$$p_d(i) = \mathbf{P}[\eta(o) = i] = \sum_{j=0}^{i} \frac{q_d(j)}{2d-j}.$$

Let us modify the bijection based on the above burning process, as follows: from vertices in $V \setminus W$, we choose an outgoing edge of the spanning tree as in Majumdar and Dhar's original bijection. We choose an outgoing edge from o to the set $V \setminus W$ according to the value of $\eta(o) \in \{\deg_W(o), \dots, 2d-1\}$ in a bijective fashion. Finally, we choose outgoing edges from vertices in W, again as in the standard burning bijection. In the resulting spanning tree we have that W equals the set of descendants of o.

For the purposes of simulating $\deg_W(o)$, first note that

$$\{y \sim o : y \in W\} \subset \{y \sim o : \mathrm{dist}(y, \rho) > \mathrm{dist}(o, \rho)\},$$

but the containment may be strict: there can exist $z \sim o$, $z \notin W$ such that $\mathrm{dist}(z, \rho) > \mathrm{dist}(o, \rho)$. In order to distinguish the vertices in W, we proceeded as follows. We first generated the LERW γ_o from o to ρ. We added a large constant SHIFT to its length, and set $d'(o) = \mathrm{dist}(o, \rho) + \mathrm{SHIFT}$. Then we generated the remaining LERWs, and computed $d'(x) = |\gamma_x| + d'(y)$, where y is the vertex in the target set of γ_x where the LERW hits. The added shift at o ensures that if $x \notin W$, then $d'(x) = \mathrm{dist}(x, \rho)$, while for $x \in W$, we have $d'(x) = \mathrm{dist}(x, \rho) + \mathrm{SHIFT}$. Choosing SHIFT sufficiently large ensures that

$$\{y \in W : y \sim o\} = \{y \sim o : d'(y) > d'(o)\},$$

and hence $\deg_W(o)$ is readily available from the simulated spanning tree. In $d = 2, 3$ we chose SHIFT to be the volume of the box $(2L)^d$, and in $d \geq 5$ we chose it to be the size of the hashtable.

2.3.1 5D variance estimate

In dimension $d = 5$, in order to only sample configurations where avalanches occur, we disregard the value of η at o, and set it equal to $2d-1$. This biases the toppling probabilities in a computable way.

Let $Q = \deg_W(o)$ and $P = \eta(o)$ be random variables, then, according to the bijection, we have

$$\mathbf{P}_L[P = j | Q = i] = \frac{1}{2d - i}, \quad 0 \leq i \leq j \leq 2d-1. \tag{2.1}$$

Let the avalanche cluster be $\mathrm{Av} := \{x \in V : x \text{ topples at least once after adding at } o\}$. Then we get the toppling probability

$$\begin{aligned}\mathbf{P}_L[x \in \mathrm{Av}] &= \mathbf{P}_L[x \in \mathrm{Av} | P = 2d-1] \times \mathbf{P}_L[P = 2d-1] \\ &= \sum_{i=0}^{2d-1} \mathbf{P}_L[x \in \mathrm{Av} | P = 2d-1, Q = i] \times \mathbf{P}_L[P = 2d-1 | Q = i] \times \mathbf{P}_L[Q = i].\end{aligned}$$

By (2.1), we have $\mathbf{P}_L[P = 2d-1 | Q = i] = 1/(2d-i)$. Let $p_L(i, x) = \mathbf{P}_L[x \in \mathrm{Av} | P = 2d-1, Q = i]$. This is estimated as follows. In each sample, we record the value of $Q = i$, set $\eta(o) = 2d-1$, add a grain at o, and simulate the avalanche. We check whether x toppled or not. Summing over all possible values of Q, we compute the toppling probability.

In order to estimate the standard error of the toppling probability estimate, let $Z_x = I[x \in \mathrm{Av}]$ be a random variable, $\mathbf{P}_L[Z_x = 1 | P = 2d-1, Q = i] = p_L(i, x)$. Conditioned on

$\{Q = i\} \cap \{P = 2d-1\}$, we define the random variable $Y_x = \frac{1}{2d-i} Z_x$. Then the adjusted toppling probability

$$\mathbf{P}_L\Big[Y_x = \frac{1}{2d-i}\Big|Q = i\Big] = p_L(i,x)$$

with the expectation and variance conditioned on Q

$$\mathbf{E}_L[Y_x|Q] = \frac{p_L(Q,x)}{2d-Q} \quad \text{and} \quad \mathbf{Var}_L(Y_x|Q) = \frac{p_L(Q,x)(1-p_L(Q,x))}{(2d-Q)^2}.$$

The toppling probability $\mathbf{P}_L[x \in \mathrm{Av}] \simeq \frac{1}{n}\sum_{k=1}^{n} Y_x^{(k)}$, where each $Y_x^{(k)}$ takes values 0 or $1/(2d-Q)$. Comparing with Z_x, we expect that the variance of Y_x is smaller than that of Z_x.

Denote $q_L(i) = \mathbf{P}_L[Q = i]$. Since $\mathbf{E}_L[Y_x] = \mathbf{E}_L[\mathbf{E}_L[Y_x|Q]] = \mathbf{P}_L[x \in \mathrm{Av}] = t_L(x;o) =: t_L(x)$ and $t_L(x) = \sum_{i=0}^{2d-1} q_L(i)\frac{p_L(i,x)}{2d-i}$, we have

$$\begin{aligned}
&\mathbf{Var}_L(\mathbf{E}_L[Y_x|Q]) = \mathbf{E}_L\Big[\frac{p_L(Q,x)^2}{(2d-Q)^2}\Big] - t_L(x)^2,\\
&\mathbf{E}_L[\mathbf{Var}_L(Y_x|Q)] = \mathbf{E}_L\Big[\frac{p_L(Q,x)(1-p_L(Q,x))}{(2d-Q)^2}\Big],\\
&\mathbf{Var}_L(Y_x) = \mathbf{E}_L(\mathbf{Var}_L(Y_x|Q)) + \mathbf{Var}_L(\mathbf{E}_L[Y_x|Q]) = \mathbf{E}_L\Big[\frac{p_L(Q,x)}{(2d-Q)^2}\Big] - t_L(x)^2\\
&\quad = \sum_{i=0}^{2d-1} q_L(i)\frac{p_L(i,x)}{(2d-i)^2} - t_L(x)^2 \le t_L(x) - t_L(x)^2 = t_L(x)(1-t_L(x)).
\end{aligned}$$

Based on the above, we recorded $\sum_{i=0}^{2d-1} \frac{\hat{p}_L(i,x)}{(2d-i)^2} - \hat{t}_L(x)^2$, where $\hat{p}$ and $\hat{t}$ denote simulation estimates. This gives an approximation to the variance of the toppling probability estimate at x.

As a comparison with simple sampling we note the following. Let $d = 5$, $L = 32$, and let x be a neighbour of the origin. Then simple sampling with 1.5×10^6 avalanches (on 64 nodes) took $16,901$ seconds of CPU time per node, resulting in the estimate $\hat{t}_L(x) = 0.0157 \pm 0.0001$ With variance reduction, the same precision was obtained with 1.5×10^5 avalanches (on 64 nodes) and took 3455 seconds of CPU time per node, with a time save of a factor 4.89.

2.3.2 Variance of height probability estimates in $d = 32$

We recorded the estimated probabilities $\hat{q}_d(i)$ for $i = 0, \ldots, 2d-1$ while simulating the height probabilities $\hat{p}_d(i)$ in $d = 32$. Then we can compute the variance of the height probability estimates as follows. We have

$$\hat{p}_d(i) = \sum_{j=0}^{i} \frac{\hat{q}_d(j)}{2d-j}, \quad i = 0, \ldots, 2d-1.$$

Since the estimates $\hat{q}_d(j)$ are almost independent, except for the constraint $\sum_{j=0}^{2d-1} \hat{q}_d(j) = 1$, the variance of the height probability estimates is

$$\mathbf{Var}(\hat{p}_d(i)) \simeq \sum_{j=0}^{i} \frac{1}{(2d-j)^2}\mathbf{Var}(\hat{q}_d(j)) = \sum_{j=0}^{i} \frac{1}{(2d-j)^2}\frac{\hat{q}_d(j)(1-\hat{q}_d(j))}{n},$$

where $i = 0, 1, \ldots, 2d-1$ and n is the number of samples generated.

2.4 Avalanche simulation

Using the Abelian property of the model, Ivashkevich, Ktitarev and Priezzhev [20] introduced a special order of topplings of non-stable vertices during an avalanche. We use this to generate the avalanche in $d = 2, 3$ and 5 as follows. First, adding a grain to o, if o is unstable, we topple it once and then topple all possible vertices without toppling o a second time. The toppled vertices form the first wave of topplings in the avalanche. Then, we allow the vertex o to topple a second time creating a second wave and so on. The process terminates when o becomes stable. Hence, we obtain the representation of the avalanche as a sequence of waves. In each wave, no vertex can topple more than once. We made use of this property as follows: whenever a vertex reached the height $2d$, we pushed it onto a stack containing vertices to be toppled, and popped from this stack until it became empty.

The avalanches are expected to behave differently in dimensions $d \geq 5$, compared to $d = 2, 3$. Long loops are unlikely, and the loop erased random walk behaves similarly to the random walk, in particular it scales diffusively [21, Section 7.7]. Also, independent random walks starting from two neighbouring vertices are likely to either meet after a few steps or not to meet at all, i.e. they are likely to connect to the sink with disjoint paths. Considering the Dirichlet boundary conditions, the number of vertices in d dimensions is $O(L^d)$ and the number of steps that the random walk takes to exit a box is $O(L^2)$. In high dimensions, the order of the number of vertices grows much faster than that of the number of steps of the random walk. Therefore, it is very inefficient to store the entire box, since we are likely to only use a small part of the box. The idea is to only generate loop erased random walks when they are needed. The way to do this is the following.

First, the loop erased random walks starting from o and its neighbours are generated. This allows the computation of the random variable Q. We then set $\eta(o) = 2d - 1$. We compute the sand heights of the neighbours by running loop erased random walks starting from their neighbours. This allows the toppling of o to be carried out. We repeat the above steps as long as there are topplings.

We used hashing [16, Sections 6.5,6.6] to store the steps of the walk in such a way that it is easy to locate intersections. We used a hash function of the form

$$f(x) = \sum_{i=1}^{2d} x_i * m^{i-1} \pmod{\text{HASHSIZE}}$$

for a point x in the box $\{1, \ldots, 2L-1\}^d$, where L, m and HASHSIZE are powers of 2.

In high dimension, avalanches are 4 dimensional and an avalanche that reaches all the way to the boundary has about $O(L^4)$ vertices. Each of these L^4 vertices will have its own random walk. This means we need at most $O(L^6)$ random walk steps to be stored, independently of the dimension. A sample was discarded when the hashtable was full.

3 2D results

3.1 Toppling probabilities in the bulk

We simulated the toppling probability both with Dirichlet and periodic boundary conditions. We found similar behaviour in different radial directions; see Figure 3. It appears that asymptotically, the toppling probability only depends on the Euclidean distance from the origin (in

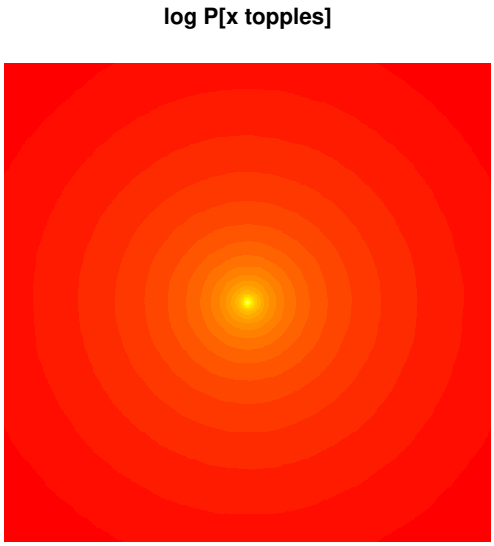

Figure 3: A heat-plot of the logarithm of the toppling probability with Dirichlet boundary conditions in $d = 2$ for a system with $L = 4096$. The values are shown for vertices in the box $[-256, 256]^2$.

the infinite volume limit). In the case of periodic boundary conditions, with the largest system size considered $L = 4096$, we occasionally encountered some extremely long avalanches.

Assuming the behaviour $t(x) := \mathbf{P}[x \text{ topples}] \sim c\,|x|^{-\eta}$ for $|x| \gg 1$ (that is, in the infinite volume limit $L \to \infty$), we want to estimate $\eta = \eta(2)$. A log-log plot of the numerical estimates $\hat{t}_L(x)$ are shown in Figure 4.

We have attempted to fit a finite-size scaling form $t_L(x) \approx c\,|x|^{-a}\, f_2(|x|/L^{1/\nu})$, with a scaling function f_2, to the data. For this, we minimized the sum of squares of the pairwise differences between $t_L(x)|x|^a$ and $t_{L'}(x')|x'|^a$, with $|x|/L^{1/\nu} = |x'|/(L')^{1/\nu}$, normalized by the standard error of the difference. First, this clearly showed that we must have $\nu = 1$. Second, we obtained a reasonable collapse of the data for $a = 0.43$, when small $|x|$ values ($|x/L| < 50/512$) were excluded from the least squares sum; see Figure 5.

Alternatively, a least squares fit of $\log \hat{t}_L(x)$ against $\log |x|$, for vertices x along the positive x-axis with $20 \le |x| \le 150$ gives the estimate $\eta(2) \approx \hat{\eta}(2) = 0.42$; see Figure 6.

Multiplying $\hat{t}_L(x)$ by $|x|^{\hat{\eta}}$ we found little deviation from a constant; see Figure 7.

We also simulated the toppling probability with periodic boundary conditions, and this gave similar results. The agreement with the power law appears to extends to a longer interval, and the estimated exponent, based on a least squares fit to the log-log data over $20 \le |x| \le 500$, gave $\hat{\eta}(2) \approx 0.41$. Figure 8 shows the toppling probabilities rescaled by $|x|^{0.41}$ in systems of size $L = 512, 1024, 2048, 4096$. Figure 9 compares the $L = 4096$ data rescaled with varying η.

The least squares fit of $\log \hat{t}_L(x)$ against $\log |x|$, for all vertices x with Euclidean distance $20 \le |x| \le 100$ gives an estimate $\hat{\eta}'(2) \approx \hat{\eta}(2)$, that is, $\hat{\eta}'(2) \approx 0.42$. Multiplying $\hat{t}_L(x)$ by $|x|^{\hat{\eta}'}$ the graph settles to be horizontal for moderate values of $|x|$; see Figure 10.

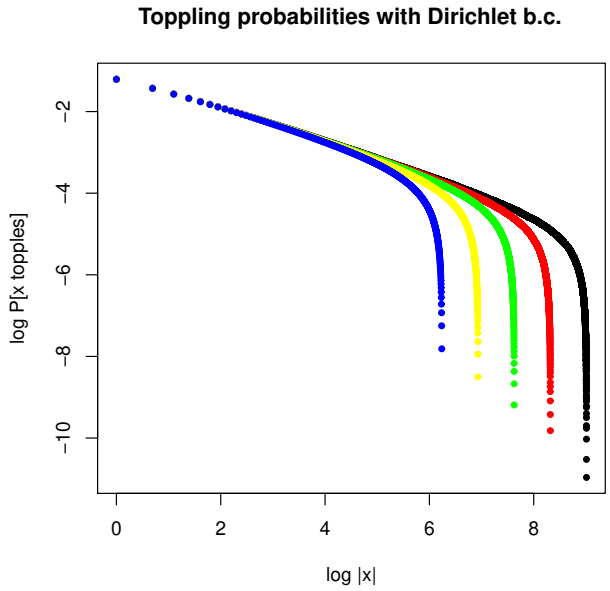

Figure 4: The logarithm of the toppling probabilities against the logarithm of $|x|$'s with Dirichlet boundary conditions in $d = 2$ for systems with $L = 512$ (blue), 1024 (yellow), 2048 (green), 4096 (red), and 8192 (black) with sample sizes 6×10^7, 3×10^7, 7.5×10^6, 4×10^6 and 10^6 respectively. The probabilities are shown for vertices in the positive x-axis up to $L-1$.

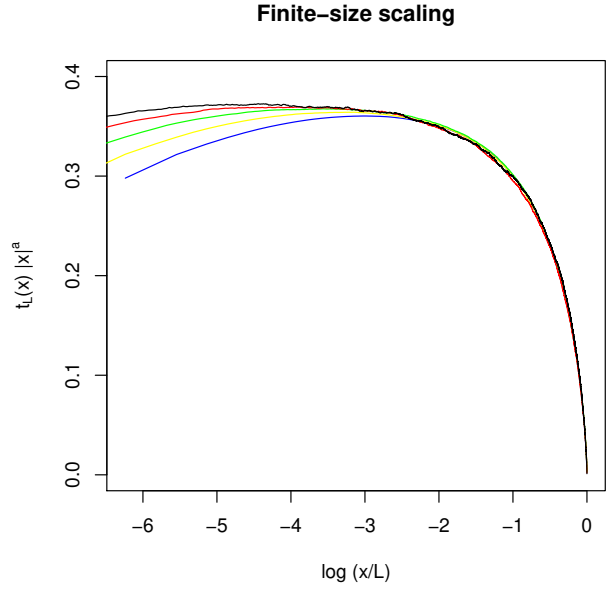

Figure 5: The estimates $\hat{t}_L(x)$ rescaled by the $|x|^a$, where $a = 0.43$ is obtained from finite scaling for $50/512 \leq |x/L| \leq 1$, when considering Dirichlet boundary conditions in $d = 2$ for systems with $L = 512$ (blue), 1024 (yellow), 2048 (green), 4096 (red), and 8192 (black). Sample sizes are as in Figure 4.

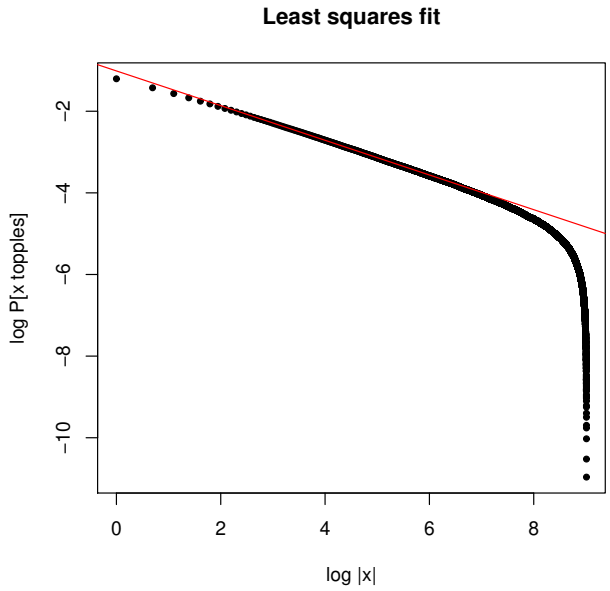

Figure 6: The logarithm of the toppling probability against the logarithm of $|x|$ with Dirichlet boundary conditions in $d = 2$ for a systems with $L = 8192$ (black dots). The probabilities are shown for vertices in the positive x-axis up to $L - 1$. The line of best fit with slope 0.42 is from the least squares method (red line).

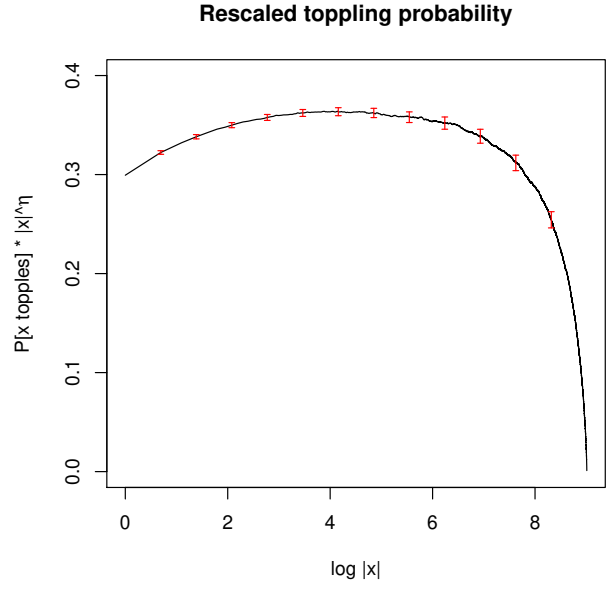

Figure 7: The toppling probability with Dirichlet boundary conditions in a system with $L = 8192$, rescaled by $|x|^{\hat{\eta}}$ ($\hat{\eta} = 0.42$) against the logarithm of $|x|$, where x is taken along the positive x-axis between 1 and $L - 1$. The error bars show ± 2 standard deviations (for every power of 2 only, for readability). The number of samples taken was 10^6.

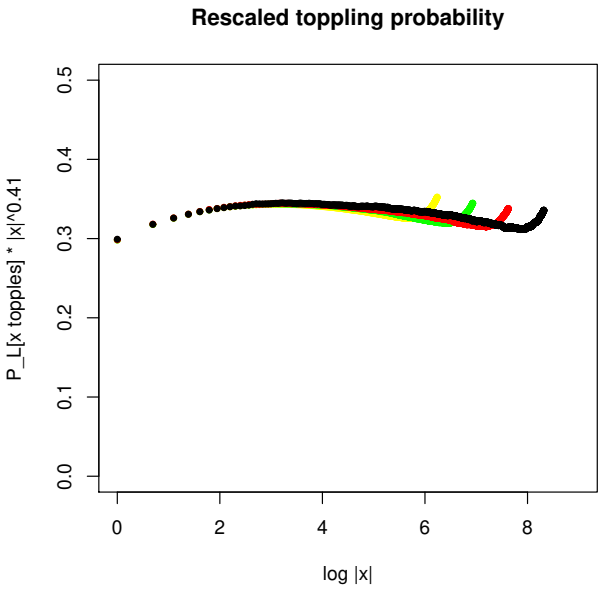

Figure 8: Rescaled toppling probabilities against the logarithm of $|x|$ with periodic boundary conditions in $d = 2$ for systems with $L = 512$ (yellow), 1024 (green), 2048 (red), and 4096 (black) (with sample sizes 2×10^7, 1.5×10^7, 3×10^6 and 7.5×10^5). The probabilities are shown for vertices in the positive x-axis up to L.

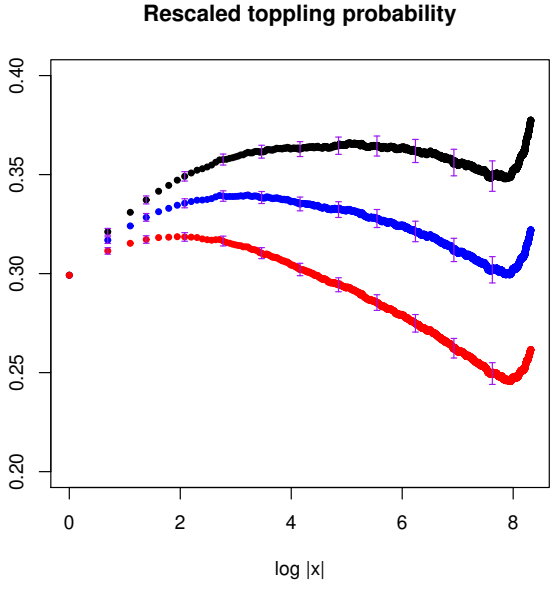

Figure 9: Toppling probabilities against the logarithm of $|x|$ with periodic boundary conditions in $d = 2$ for a system with $L = 4096$ rescaled by $|x|^\eta$ with $\eta = \hat{\eta} \approx 0.425$ (black), $\eta = 0.405$ (blue), $\eta = 0.38$ (red). The probabilities are shown for vertices in the positive x-axis up to L. Error bars (green) shown for $|x|$ a power of 2.

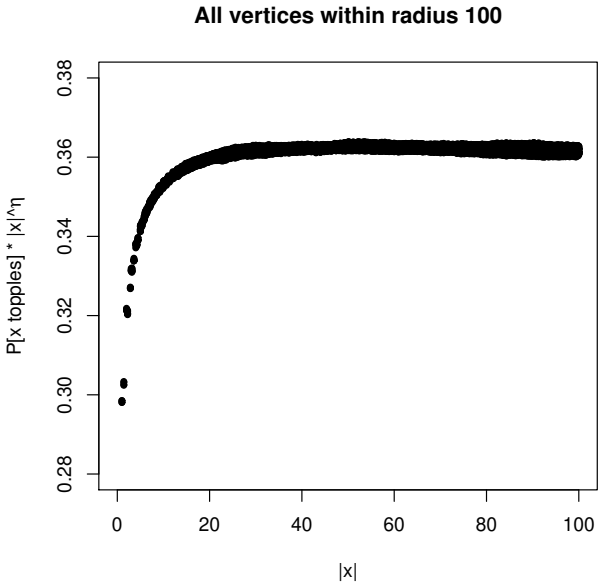

Figure 10: The toppling probability with Dirichlet boundary conditions in $d = 2$ for a system with $L = 4096$, rescaled by $|x|^{\hat{\eta}}$ ($\hat{\eta} = 0.42$). The probabilities are shown for all vertices in a disk of radius 100.

Based on the above, we make the following conjecture for the toppling probability in the infinite volume limit $L \to \infty$:

$$\mathbf{P}[x \text{ topples}] = |x|^{-\eta+o(1)},$$

where $\eta = \eta(2) = 0.4 \pm 0.03$.

Toppling probabilities in the scaling limit. Finally, we comment on the toppling probability of those vertices x whose distance from the origin is of the same order as L. Rescaling by $|x|^{\hat{a}}$, where $\hat{a} = 0.43$ was obtained from the finite-size scaling analysis, and plotting against $|x|/L$, yields the graph in Figure 11. The graph suggests that as long as $|x|/L$ is bounded away from 0, the rescaled quantity $t_L(x)|x|^a$ has a scaling limit $f_2(y)$, as $x/L \to y \in [-1, 1]^2$.

3.2 The number of waves in 2D

In this section we present results on the number of waves in avalanches initiated at the origin. The distribution of the number of waves is the most interesting in 2D, since the average number of waves diverges logarithmically as $L \to \infty$:

$$\mathbf{E}_L[\text{number of waves}] = G_L(o, o) \sim \frac{1}{2\pi} \log L, \quad \text{as } L \to \infty. \tag{3.1}$$

Recalling that $n(o, o)$ denotes the number of topplings at o caused by addition of a grain at o, let us put

$$w_L(n) = \mathbf{P}_L[n(o, o) = n], \qquad w(n) = \lim_{L\to\infty} w_L(n).$$

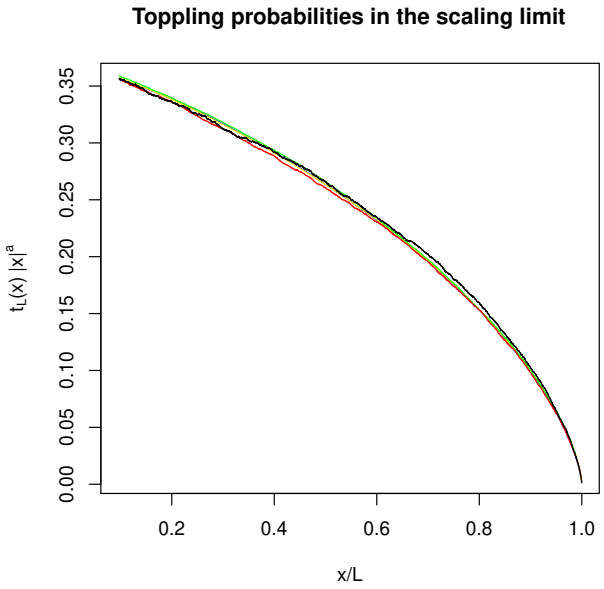

Figure 11: The rescaled toppling probability with Dirichlet boundary conditions in $d = 2$ for systems with $L = 512$ (yellow), 1024 (green), 2048 (red), and 4096 (black). The probabilities are shown for points on the positive x-axis with $50/512 \leq |x/L| \leq 1$.

(The existence of the limit defining $w(n)$ is known rigorously; see [22].) Let us define the complementary distribution functions

$$W_L(n) = \mathbf{P}_L[n(o,o) \geq n] = \sum_{m \geq n} w_L(m) \qquad \text{and} \qquad W(n) = \mathbf{P}[n(o,o) \geq n] = \sum_{m \geq n} w(m).$$

Assuming that $w(n)$ decays as a power law: $w(n) \approx n^{-\delta}$, and from the divergence of the mean as in (3.1), it has been predicted that $W(n) \approx n^{-1}$ (and hence $\delta = 2$); see [4, Eqn. (5.11)].

In Figure 12 we show for $L = 8192$ the rescaled quantity $w_L(n)n^2$. Error bars are shown up to $n = 200$. Beyond this bound, avalanches with particular values of n are too infrequent to estimate from our data. There is no clear indication of the rescaled values settling down to a constant for moderate n.

The data is a lot smoother for $W_L(n)$, and the errors for the rescaled quantity $W_L(n)n$ are also smaller. In Figure 13 we show for $L = 8192$ the rescaled quantity $W_L(n)n$ against $\log n$ for $1 \leq n \leq 2000$. It is apparent that the graph does not settle to a constant value for moderate values of n. Therefore, if $W(n)$ indeed satisfies an asymptotic of the form $W(n) \sim cn^{-1}$, convergence to this asymptotic is reached only for very large values of L and n. It has been pointed out in [7] that the simulation data in that paper better fits with $\delta \approx 2.1$. However, any exponent > 2 can be ruled out, as

$$\sum_{n \geq 1} nw(n) = \lim_{L \to \infty} G_L(o,o) = \infty. \tag{3.2}$$

An alternative possibility is that the scaling behaviour of $W_L(n)$ depends in a more complicated way on L and n. For example, it is consistent with (3.2) to have $W(n) \sim cn^{-1}(\log n)^{-\beta}$ with

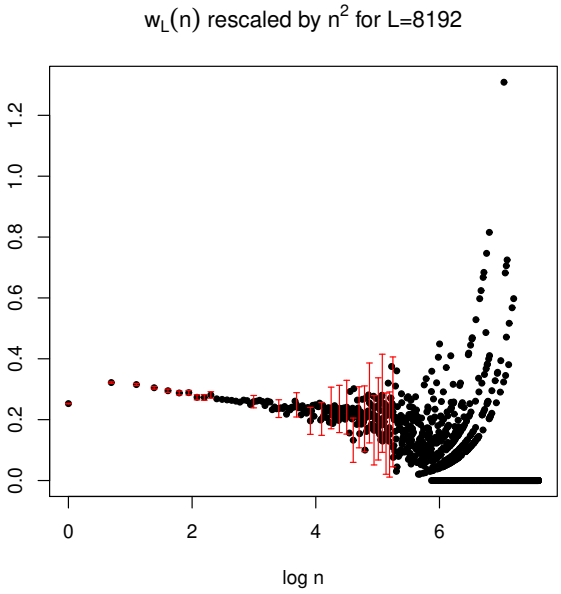

Figure 12: $w_L(n)\, n^2$ with Dirichlet boundary conditions in $d = 2$, when considering $L = 8192$, against $\log n$ for $1 \leq n \leq 2000$. Error bars show ± 2 standard deviations. The sample size is 10^6.

some $0 < \beta < 1$. Note that we cannot have $W_L(n)$ satisfy this behaviour with a cut-off at some L^σ, since[1]

$$\sum_{n=2}^{L^\sigma} \frac{1}{n \, \log^\beta n} \sim c(\sigma) \, (\log L)^{1-\beta}$$

Hence a logarithmic correction of the form above would require that for finite L there is sufficient weight on very large avalanches (whose size diverges with L) to yield $G_L(o, o) \sim (2\pi)^{-1} \log L$. In Figure 14, we show the effect of scaling the data with different powers $(\log n)^\beta$. Scaling with $\beta = 0.4$ describes the data fairly well for moderate values of n. However, our conclusion from the above is that understanding the scaling of $w(n)$ or $W(n)$ requires further work.

4 3D results

In $3D$ we found that with periodic boundary conditions there were some extremely long avalanches. In this paper we only include our data with Dirichlet boundary conditions. Assuming the behaviour $t(x) \sim c\,|x|^{-1-\eta}$ in the infinite volume limit $L \to \infty$, we want to estimate $\eta = \eta(3)$. A log-log plot of the numerical estimates $\hat{t}_L(x)$ are shown in Figure 15.

Fitting a finite size-scaling form $t_L(x) = |x|^{-1-a} f_3(|x|/L)$ yielded $a \approx 0.0$, when small values of x (those with $|x|/L < 5/32$) were excluded; see Figure 16.

On the other hand, for the largest system size ($L = 256$), the least squares fit of $\log \hat{t}_L(x)$ against $\log |x|$, for vertices x along the positive x-axis with $7 \leq |x| \leq 55$ gives the somewhat different estimate $\eta(3) \approx \hat{\eta}(3) = 0.09$; see Figure 17.

[1] We thank an anonymous referee for calling our attention to this.

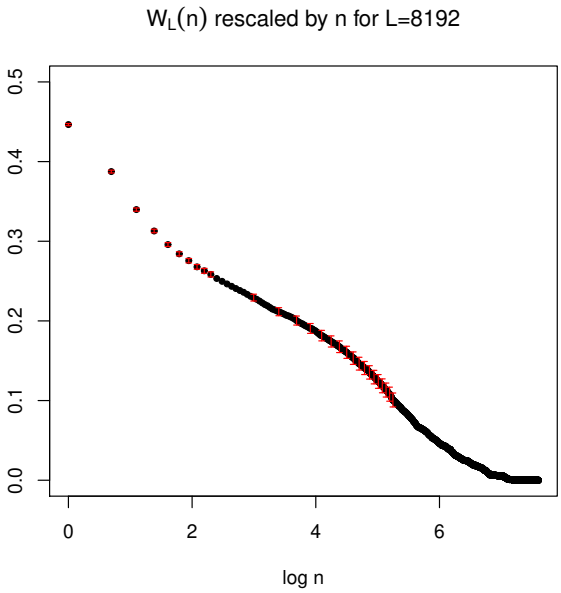

Figure 13: $W_L(n)\, n$ with Dirichlet boundary conditions in $d = 2$, when considering $L = 8192$, against $\log n$ for $1 \leq n \leq 2000$. Error bars show ± 2 standard deviations. The sample size is 10^6.

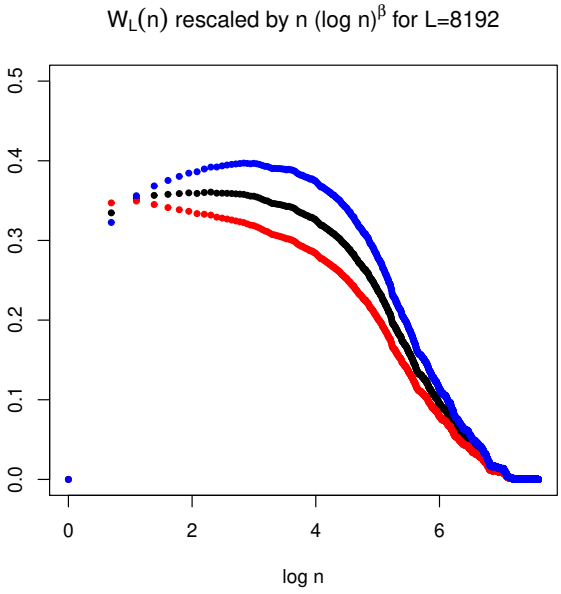

Figure 14: $W_L(n)\, n\, (\log n)^{\beta}$, with Dirichlet boundary conditions in $d = 2$, when considering $L = 8192$, for $\beta = 0.3$ (red), $\beta = 0.4$ (black), $\beta = 0.5$ (blue). The horizontal axis shows $\log n$ for $1 \leq n \leq 2000$.

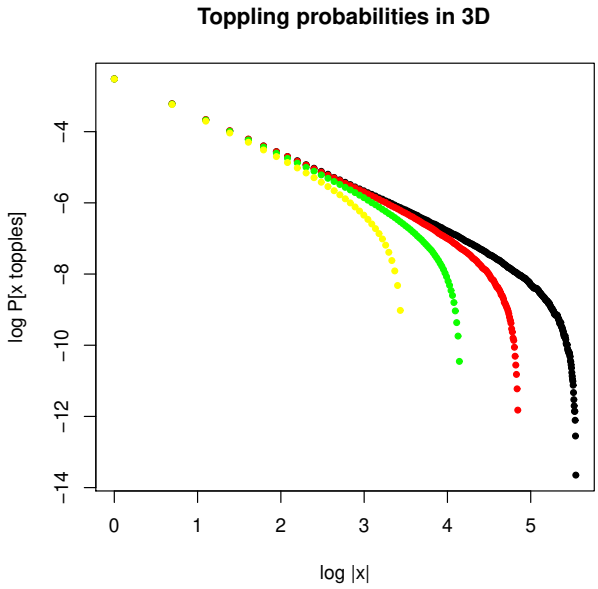

Figure 15: The logarithm of the toppling probabilities against the logarithm of $|x|$'s with Dirichlet boundary conditions in $d = 3$ for systems with $L = 32$ (yellow), 64 (green), 128 (red), and 256 (black) (with sample sizes 8×10^7, 2×10^7, 4.5×10^6, 4×10^6).

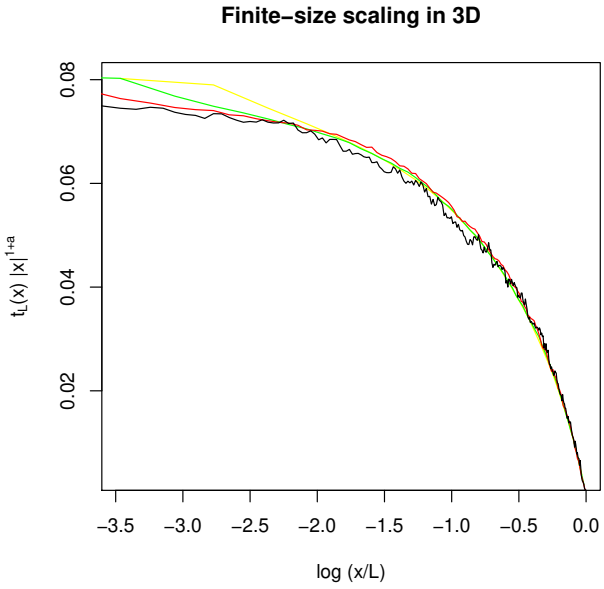

Figure 16: The estimates $\hat{t}_L(x)$ rescaled by the $|x|^{1+a}$, where $a = 0.0$ is obtained from finite scaling for $5/32 \leq |x/L| \leq 1$, when considering Dirichlet boundary conditions in $d = 3$ for systems with $L = 32$ (yellow), 64 (green), 128 (red), and 256 (black).

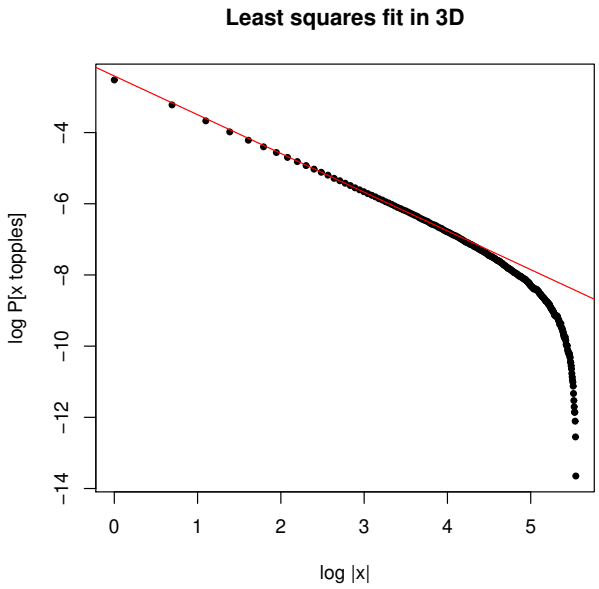

Figure 17: The logarithm of the toppling probability against the logarithm of $|x|$ with Dirichlet boundary conditions in a systems with $L = 256$ (black dots). The line of best fit with slope $1 + \hat{\eta}$, where $\hat{\eta} = 0.09$, from the least squares method (red line).

The estimate $\hat{t}_L(x)$ rescaled by $|x|^{1+\hat{\eta}}$ appear to approach a constant with little deviation; see Figure 18.

Based on the above, we believe that the exponent describing the toppling probability in the infinite volume limit differs from the one describing it in the scaling limit $x/L \to y$. We make the following conjecture:

$$\mathbf{P}[x \text{ topples}] = |x|^{-1-\eta+o(1)}$$

with $\eta = \eta(3) \approx 0.1$.

Toppling probabilities in the scaling limit. We comment on the toppling probability of those vertices x whose distance from the origin is of the same order as L. Rescaling by $|x|^{1+\hat{a}}$, where $\hat{a} = 0.0$ was obtained from the finite-size scaling analysis, and plotting against $|x|/L$, yields the graph in Figure 19. The graph suggests that as long as $|x|/L$ is bounded away from 0, the rescaled quantity $t_L(x)|x|^{1+a}$ has a scaling limit $f_3(y)$, as $x/L \to y \in [-1, 1]^3$.

From the assumed scaling form $t_L(x) = |x|^{-1-a} f_3(x/L)$, the difference of logarithms

$$\frac{1}{\log 2} \left(\log t_L(x) - \log t_{2L}(2x) \right) \approx a.$$

We show these differences in Figure 20 for $L = 128, 64, 32$, together with the horizontal line corresponding to $a = 0.0$.

The above raises the question: if you rescale with $|x|$, does the limit exist? In other words: is there a function $f_3 : [-1, 1]^3 \to \mathbb{R}$ such that

$$|x| \mathbf{P}_L[x \text{ topples}] \sim f_3(x/L), \quad \text{as } L \to \infty?$$

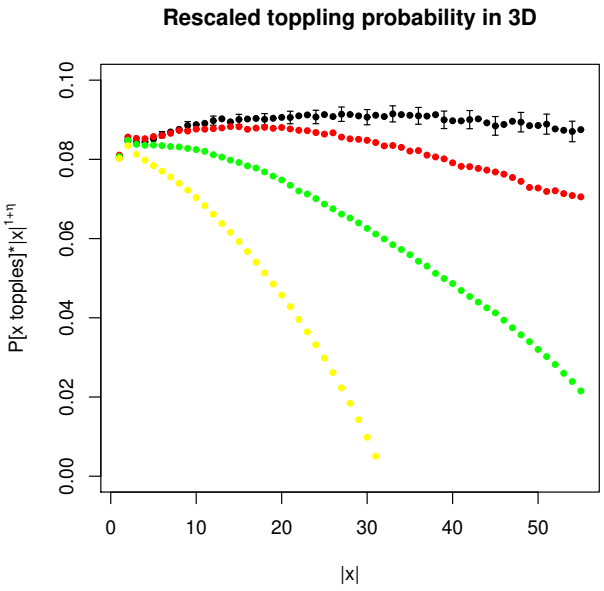

Figure 18: The toppling probability with Dirichlet boundary conditions in systems with $L = 32$ (yellow), 64 (green), 128 (red), and 256 (black), rescaled by $|x|^{1+\hat{\eta}}$, where x is taken along the positive x-axis between 1 and 55, and $\hat{\eta} \approx 0.1$. The error bars show ± 2 standard deviations of the toppling probability with $L = 256$ (for every 3-rd point only, for readability). Sample sizes are same as in Figure 15.

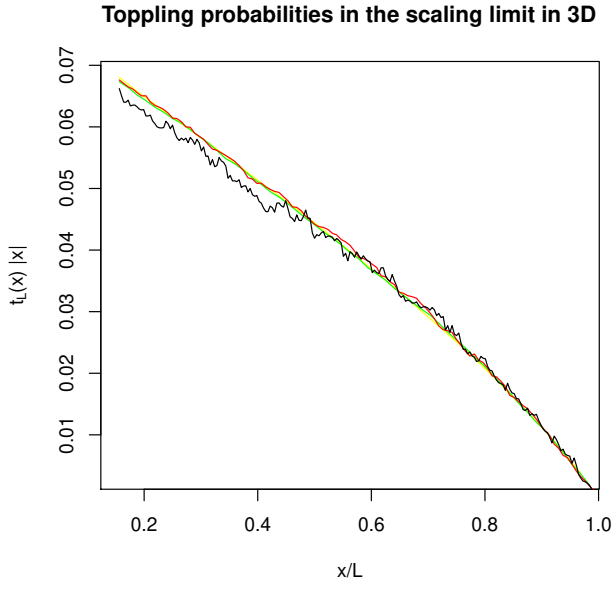

Figure 19: The rescaled toppling probability $t_L(x)|x|$ with Dirichlet boundary conditions in $d = 3$ for systems with $L = 32$ (yellow), 64 (green), 128 (red), and 256 (black). The probabilities are shown for points on the positive x-axis with $5/32 \leq |x/L| \leq 1$.

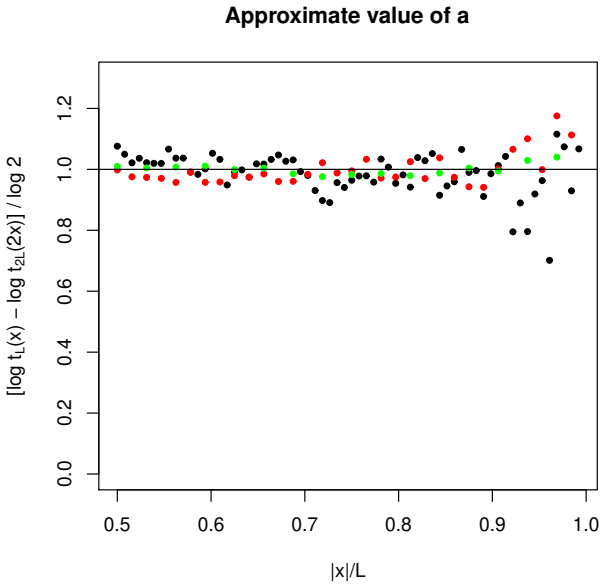

Figure 20: The difference of logarithms in $d = 3$ for $L = 32$ (green), 64 (red), and 128 (black). A horizontal line with $y = 1$ (black line), corresponding to $a = 0$.

5 High-dimensional results

5.1 Toppling probability simulations in 5D

In dimensions $d \geq 5$, it has been proved [5] that $\eta = \eta(d) = 0$, in the sense that

$$c|x|^{2-d} \leq \mathbf{P}[x \text{ topples}] \leq C|x|^{2-d}.$$

Based on this we can expect that the toppling probability (in the infinite volume limit $L \to \infty$) rescaled by $|x|^{d-2}$ is asymptotic to a constant as $|x| \to \infty$. Figure 21 shows our simulation results which appear consistent with this conjecture.

5.2 Asymptotic height probabilities

Recall that $p_d(i) = \mathbf{P}[\eta(o) = i]$ denotes the height probability in d dimensions (in the infinite volume limit $L \to \infty$). The following theorem states the asymptotic form of the height probabilities as $d \to \infty$. The proof of this theorem, that relies on analyzing Wilson's algorithm on the infinite graph $\mathbb{Z}^d$, will be published separately from the present paper [23].

Theorem 5.1. *(i) For $0 \leq i \leq d^{1/2}$, we have*

$$p_d(i) = \sum_{j=0}^{i} \frac{e^{-1}\frac{1}{j!}}{2d-j} + O\Big(\frac{i}{d^2}\Big) = \frac{1}{2d}\sum_{j=0}^{i} e^{-1}\frac{1}{j!} + O\Big(\frac{i}{d^2}\Big).$$

(ii) If $d^{1/2} < i \leq 2d-1$, we have

$$p_d(i) = p_d(d^{1/2}) + O(d^{-3/2}).$$

In particular, $p_d(i) \sim (2d)^{-1}$, if $i, d \to \infty$.

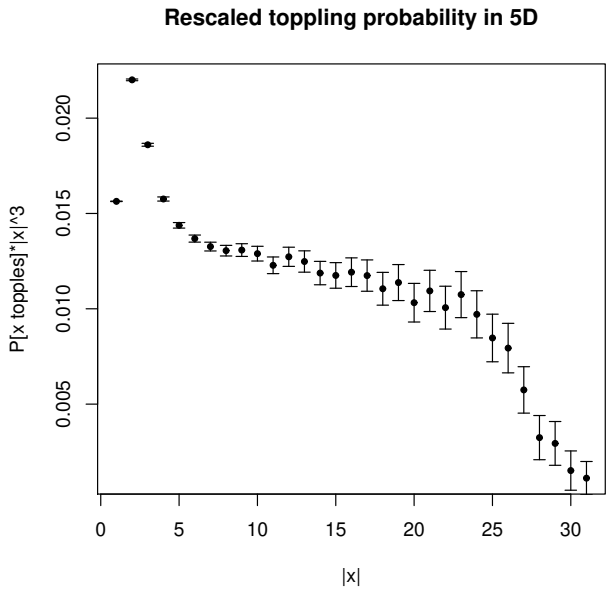

Figure 21: The toppling probability in the box with radius $L = 32$ in 5D, rescaled by $|x|^{d-2}$, where x is taken along the first coordinate axis. The error bars show ± 2 standard deviations. The number of samples taken was 4×10^7, with approximately 400 samples discarded due to a full hashtable.

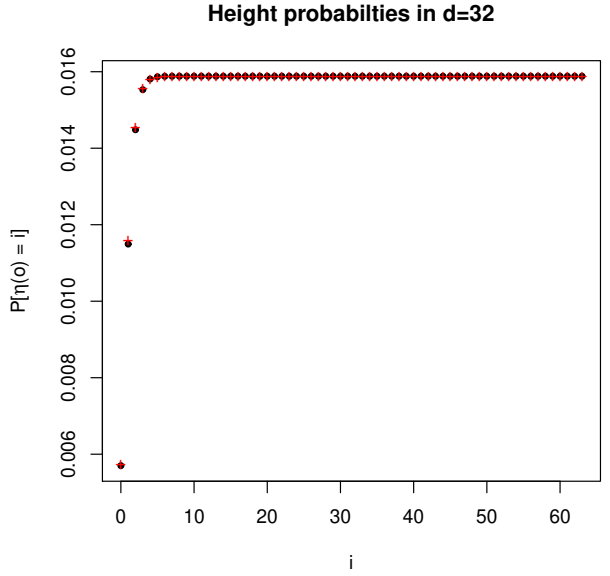

Figure 22: Simulated height probabilities (black dots) in $d = 32$ for a system with $L = 128$ (with sample size 4×10^6), and the asymptotic formula (red pluses).

The asymptotic formula appearing in part (i) of the theorem is the same as obtained by Dhar and Majumdar [10] on the Bethe lattice with large coordination number. Figure 22 compares the formula to simulations in $d = 32$ in the finite volume $L = 128$.

Acknowledgements. We thank two anonymous referees for their constructive criticism.

References

[1] Bak P, Tang C and Wiesenfeld K, *Self-organized criticality: An explanation of the* $1/f$ *noise,* 1987 *Phys. Rev. Lett.* **59** 381

[2] Dhar D, *Theoretical studies of self-organized criticality,* 2006 *Phys. A (Amsterdam, Neth.)* **369** 29

[3] Dhar D, *Self-organized critical state of sandpile automation models,* 1990 *Phys. Rev. Lett.* **64** 1613

[4] Majumdar S N and Dhar D, *Equivalence between the abelian sandpile model and the* $q \to 0$ *limit of the Potts model,* 1992 *Phys. A (Amsterdam, Neth.)* **185** 129

[5] Jarai A A, Redig F and Saada E, *Approaching criticality via the zero dissipation limit in the abelian avalanche model,* 2015 *J. Stat. Phys.* **159** 1369

[6] Manna S S, *Large-scale simulation of avalanche cluster distribution in sand pile model* 1990 *J. Stat. Phys.* **59** 509

[7] Grassberger P and Manna S S, *Some more sandpiles,* 1990 *J. Phys. (Paris)* **51** 1077

[8] Priezzhev V B, *Structure of two-dimensional sandpile. I. Height probabilities,* 1994 *J. Stat. Phys.* **74** 955

[9] Ktitarev D V, Lubeck S, Grassberger P and Priezzhev V B, *Scaling of waves in the Bak-Tang-Wiesenfeld sandpile model,* 2000 *Phys. Rev. E: Stat. Phys., Plasmas, Fluids, Relat. Interdiscip. Top.* **61** 81

[10] Dhar D and Majumdar S N, *Abelian sandpile model on the bethe lattice,* 1990 *J. Phys. A: Math. Gen.* **23** 4333

[11] Wilson D B, *Generating random spanning trees more quickly than the cover time,* 1996 *Proceedings of the twenty-eight annual acm symposium on the theory of computing,* 296

[12] Matsumoto M and Nishimura T, *Mersenne twister: a* 623*-dimensionally equidistributed uniform pseudo-random number generator,* 1998 *ACM. T. Model. Comput. S.* **8** 3

[13] Haramoto H, Matsumoto M, Nishimura T, Panneton F and L'Ecuyer P, *Efficient jump ahead for* $\mathbb{F}_2$*-linear random number generators,* 2008 *INFORMS. J. Comput* **20** 385

[14] Levin D A, Peres Y and Wilmer E L, *Markov chains and mixing times,* 2009 *American Mathematical Society.*

[15] Priezzhev V B, *The upper critical dimension of the abelian sandpile model,* 2000 *J. Stat. Phys.* **98** 667

[16] Kernighan, B W, and Ritchie D M, *The C Programming Language,* 1988 *2nd. ed., Prentice Hall.*

[17] Jeng M, Piroux G and Ruelle P, *Height variables in the abelian sandpile model: scaling fields and correlations,* 2006 *J. Stat. Mech.: Theory Exp.* **2006** 10015

[18] Poghosyan V S, Priezzhev V B and Ruelle P, *Return probability for the loop-erased random walk and mean height in the Abelian sandpile model: A proof,* 2011 *J. Stat. Mech.: Theory Exp.* **2011** 12

[19] Kenyon R W and Wilson D B, *Spanning trees of graphs on surfaces and the intensity of loop-erased random walk on planar graphs,* 2015 *J. Am. Math. Sco.* **28** 985

[20] Ivashkevich E V, Ktitarev D V and Priezzhev V B, *Waves of topplings in an abelian sandpile* 1994 *Phys. A (Amsterdam, Neth.)* **209** 347

[21] Lawler G F, *Intersections of Random Walks,* 2013 *Springer New York: Imprint: Birkhauser.*

[22] Bhupatiraju S, Hanson J and Jarai A A, *Inequalities for critical exponents in d-dimensional sandpiles,* 2017 *Electron. J. Probab.* **22** 85

[23] Jarai A A and Sun M, *Asymptotic height distribution in high-dimensional sandpiles,* 2019 *In preparation.*